Performance of Three-Dimensional Graded ADI-FDTD Algorithm

Enqiu Hu and Wolfgang J.R. Hoefer

Computational Electromagnetics Research Laboratory, Department of Electrical & Computer Engineering, University of Victoria, POB 3055, Victoria, British Columbia V8W 3P6, Canada

***Abstract* — In this paper, a 3D unconditionally stable ADI-FDTD algorithm without the CFL stability constraint is described. We have investigated the computational accuracy and the CPU time of this method and compared it with conventional FDTD for both uniform and graded meshes. Since the ADI-FDTD algorithm is unconditionally stable, the selection of the time step is not restricted by stability considerations, but the relative error of the ADI-FDTD algorithm increases with increasing time step. The numerical results show that the saving in CPU time of the ADI-FDTD is not dramatic in comparison with the conventional FDTD algorithm when the mesh size and computational accuracy of both methods are the same. The reduction in the number of time steps and hence, CPU time, is offset by reduced accuracy. Therefore, the choice of the ADI-FDTD method is governed by the acceptable error.**

I. INTRODUCTION

The finite–difference time–domain (FDTD) method is a popular method due to its versatility and ability to provide accurate predictions of electromagnetic field behavior. The maximum time step is limited by the minimum spatial discretization interval as defined by the Courant-Friedrich-Levy (CFL) stability condition. However, there are some important potential applications of the FDTD technique where the CFL stability constraint is too restrictive, particularly when the cell size needed to resolve the finest geometric detail is very small.

The non-uniform grid FDTD algorithm is able to handle such situations since it can easily conform to such fine scale geometric details without substantially increasing the overall mesh size and without losing computational accuracy. However, the CFL stability constraint cannot be relaxed. The maximum time step Δt_{max} is still determined by the minimum spatial cell size. The $\Delta t_{max,}$ in turn, determines the total number of time step needed to complete the simulation.

To circumvent the stability constraint, the alternating direction implicit finite-difference time-domain (ADI-FDTD) method has recently been introduced for solving electromagnetic wave problems [1-3]. The scheme is based on an alternating direction implicit technique and the conventional FDTD algorithm. Since this method is unconditionally stable, the time step can be arbitrarily chosen without regard for the CFL constraint [2,3]. This technique has thus the potential to cut the number of time step by several orders of magnitude. Unfortunately, the simulating accuracy will decrease with increasing time step. We therefore decided to investigate the computational accuracy and CPU time of the ADI-FDTD algorithm and to compare them with the performance of the conventional FDTD algorithm. Both uniform and non-uniform (graded) meshes were employed in this study.

II. THEORETICAL FORMULATION

The non-uniform FDTD algorithm is based on a discretization of Maxwell's equations in their integral form in the non-uniform grid shown in Fig. 1.

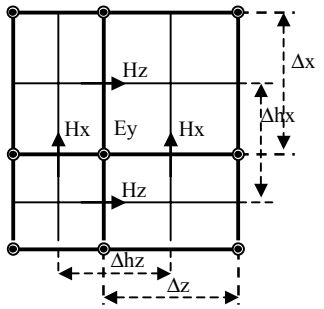

Fig. 1. Non-uniform discretization grid in two-dimension

In the ADI-FDTD algorithm, the conventional FDTD update procedure leading from the *n*th time step to the (*n+1*)th time step is broken up into two sub-steps. All field components are computed with these two sub-steps:

(1) The first sub-step: The updating equations from the *n*th time step to the (*n+1/2*)th time step are:

$$E_x\Big|_{i+1/2,j,k}^{n+1/2} = C_a\Big|_{i+1/2,j,k} E_x\Big|_{i+1/2,j,k}^{n} + C_b\Big|_{i+1/2,j,k} \left[\frac{H_z\Big|_{i+1/2,j+1/2,k}^{n+1/2} - H_z\Big|_{i+1/2,j-1/2,k}^{n+1/2}}{\Delta hy_{i+1/2,j,k}} - \frac{H_y\Big|_{i+1/2,j,k+1/2}^{n} - H_y\Big|_{i+1/2,j,k-1/2}^{n}}{\Delta hz_{i+1/2,j,k}} \right] \tag{1a}$$

$$E_y\Big|_{i,j+1/2,k}^{n+1/2} = C_a\Big|_{i,j+1/2,k} E_y\Big|_{i,j+1/2,k}^{n} + C_b\Big|_{i,j+1/2,k}$$
$$\left[\frac{H_x\Big|_{i,j+1/2,k+1/2}^{n+1/2} - H_x\Big|_{i,j+1/2,k-1/2}^{n+1/2}}{\Delta hz_{i,j+1/2,k}} - \frac{H_z\Big|_{i+1/2,j+1/2,k}^{n} - H_z\Big|_{i-1/2,j+1/2,k}^{n}}{\Delta hx_{i,j+1/2,k}}\right] \quad (1b)$$

$$E_z\Big|_{i,j,k+1/2}^{n+1/2} = C_a\Big|_{i,j,k+1/2} E_z\Big|_{i,j,k+1/2}^{n} + C_b\Big|_{i,j,k+1/2}$$
$$\left[\frac{H_y\Big|_{i+1/2,j,k+1/2}^{n+1/2} - H_y\Big|_{i-1/2,j,k+1/2}^{n+1/2}}{\Delta hx_{i,j,k+1/2}} - \frac{H_x\Big|_{i,j+1/2,k+1/2}^{n} - H_x\Big|_{i,j-1/2,k+1/2}^{n}}{\Delta hy_{i,j,k+1/2}}\right] \quad (1c)$$

$$H_x\Big|_{i,j+1/2,k+1/2}^{n+1/2} = D_a\Big|_{i,j+1/2,k+1/2} H_x\Big|_{i,j+1/2,k+1/2}^{n} + D_b\Big|_{i,j+1/2,k+1/2}$$
$$\left[\frac{E_y\Big|_{i,j+1/2,k+1}^{n+1/2} - E_y\Big|_{i,j+1/2,k}^{n+1/2}}{\Delta z_{i,j+1/2,k+1/2}} - \frac{E_z\Big|_{i,j+1,k+1/2}^{n} - E_z\Big|_{i,j,k+1/2}^{n}}{\Delta y_{i,j+1/2,k+1/2}}\right] \quad (1d)$$

$$H_y\Big|_{i+1/2,j,k+1/2}^{n+1/2} = D_a\Big|_{i+1/2,j,k+1/2} H_y\Big|_{i+1/2,j,k+1/2}^{n} + D_b\Big|_{i+1/2,j,k+1/2}$$
$$\left[\frac{E_z\Big|_{i+1,j,k+1/2}^{n+1/2} - E_z\Big|_{i,j,k+1/2}^{n+1/2}}{\Delta x_{i+1/2,j,k+1/2}} - \frac{E_x\Big|_{i+1/2,j,k+1}^{n} - E_x\Big|_{i+1/2,j,k}^{n}}{\Delta z_{i+1/2,j,k+1/2}}\right] \quad (1e)$$

$$H_z\Big|_{i+1/2,j+1/2,k}^{n+1/2} = D_a\Big|_{i+1/2,j+1/2,k} H_z\Big|_{i+1/2,j+1/2,k}^{n} + D_a\Big|_{i+1/2,j+1/2,k}$$
$$\left[\frac{E_x\Big|_{i+1/2,j+1,k}^{n+1/2} - E_x\Big|_{i+1/2,j,k}^{n+1/2}}{\Delta y_{i+1/2,j+1/2,k}} - \frac{E_y\Big|_{i+1,j+1/2,k}^{n} - E_y\Big|_{i,j+1/2,k}^{n}}{\Delta x_{i+1/2,j+1/2,k}}\right] \quad (1f)$$

where

$$C_a\Big|_{i,j,k} = \frac{2\varepsilon_{i,j,k} - \sigma_{i,j,k}\Delta t}{2\varepsilon_{i,j,k} + \sigma_{i,j,k}\Delta t} \qquad C_b\Big|_{i,j,k} = \frac{\Delta t}{2\varepsilon_{i,j,k} + \sigma_{i,j,k}\Delta t}$$

$$D_b\Big|_{i,j,k} = 1 \qquad D_b\Big|_{i,j,k} = \frac{\Delta t}{2\mu_{i,j,k}}$$

In each of the above equations, the first finite-difference on the right-hand side is evaluated implicitly from unknown field data at the same time step *n+1/2* as for the left-hand side field component, while the second finite-difference on the right-hand side is evaluated explicitly from known field data at the time step *n*.

(2) The second sub-step: The updating equations from the (*n+1/2*)th time step to the (*n+1*)th time step are:

$$E_x\Big|_{i+1/2,j,k}^{n+1} = C_a\Big|_{i+1/2,j,k} E_x\Big|_{i+1/2,j,k}^{n+1/2} + C_b\Big|_{i+1/2,j,k}$$
$$\left[\frac{H_z\Big|_{i+1/2,j+1/2,k}^{n+1/2} - H_z\Big|_{i+1/2,j-1/2,k}^{n+1/2}}{\Delta hy_{i+1/2,j,k}} - \frac{H_y\Big|_{i+1/2,j,k+1/2}^{n+1} - H_y\Big|_{i+1/2,j,k-1/2}^{n+1}}{\Delta hz_{i+1/2,j,k}}\right] \quad (2a)$$

$$E_y\Big|_{i,j+1/2,k}^{n+1} = C_a\Big|_{i,j+1/2,k} E_y\Big|_{i,j+1/2,k}^{n+1/2} + C_b\Big|_{i,j+1/2,k}$$
$$\left[\frac{H_x\Big|_{i,j+1/2,k+1/2}^{n+1/2} - H_x\Big|_{i,j+1/2,k-1/2}^{n+1/2}}{\Delta hz_{i,j+1/2,k}} - \frac{H_z\Big|_{i+1/2,j+1/2,k}^{n+1} - H_z\Big|_{i-1/2,j+1/2,k}^{n+1}}{\Delta hx_{i,j+1/2,k}}\right] \quad (2b)$$

$$E_z\Big|_{i,j,k+1/2}^{n+1} = C_a\Big|_{i,j,k+1/2} E_z\Big|_{i,j,k+1/2}^{n+1/2} + C_b\Big|_{i,j,k+1/2}$$
$$\left[\frac{H_y\Big|_{i+1/2,j,k+1/2}^{n+1/2} - H_y\Big|_{i-1/2,j,k+1/2}^{n+1/2}}{\Delta hx_{i,j,k+1/2}} - \frac{H_x\Big|_{i,j+1/2,k+1/2}^{n+1} - H_x\Big|_{i,j-1/2,k+1/2}^{n+1}}{\Delta hy_{i,j,k+1/2}}\right] \quad (2c)$$

$$H_x\Big|_{i,j+1/2,k+1/2}^{n+1} = D_a\Big|_{i,j+1/2,k+1/2} H_x\Big|_{i,j+1/2,k+1/2}^{n+1/2} + D_b\Big|_{i,j+1/2,k+1/2}$$
$$\left[\frac{E_y\Big|_{i,j+1/2,k+1}^{n+1/2} - E_y\Big|_{i,j+1/2,k}^{n+1/2}}{\Delta z_{i,j+1/2,k+1/2}} - \frac{E_z\Big|_{i,j+1,k+1/2}^{n+1} - E_z\Big|_{i,j,k+1/2}^{n+1}}{\Delta y_{i,j+1/2,k+1/2}}\right] \quad (2d)$$

$$H_y\Big|_{i+1/2,j,k+1/2}^{n+1} = D_a\Big|_{i+1/2,j,k+1/2} H_y\Big|_{i+1/2,j,k+1/2}^{n+1/2} + D_b\Big|_{i+1/2,j,k+1/2}$$
$$\left[\frac{E_z\Big|_{i+1,j,k+1/2}^{n+1/2} - E_z\Big|_{i,j,k+1/2}^{n+1/2}}{\Delta x_{i+1/2,j,k+1/2}} - \frac{E_x\Big|_{i+1/2,j,k+1}^{n+1} - E_x\Big|_{i+1/2,j,k}^{n+1}}{\Delta z_{i+1/2,j,k+1/2}}\right] \quad (2e)$$

$$H_z\Big|_{i+1/2,j+1/2,k}^{n+1} = D_a\Big|_{i+1/2,j+1/2,k} H_z\Big|_{i+1/2,j+1/2,k}^{n+1/2} + D_b\Big|_{i+1/2,j+1/2,k}$$
$$\left[\frac{E_x\Big|_{i+1/2,j+1,k}^{n+1/2} - E_x\Big|_{i+1/2,j,k}^{n+1/2}}{\Delta y_{i+1/2,j+1/2,k}} - \frac{E_y\Big|_{i+1,j+1/2,k}^{n+1} - E_y\Big|_{i,j+1/2,k}^{n+1}}{\Delta x_{i+1/2,j+1/2,k}}\right] \quad (2f)$$

In each of the above equations, the second finite-difference on the right-hand side is evaluated implicitly from as-yet unknown field data at the same time step (*n+1*) of the left-hand side field component, while the first finite-difference on the right-hand side is evaluated explicitly from known field data at the time step *n+1/2* previously computed using (1).

The system of equations summarized above for each sub-step cannot be directly used for numerical computation because some field components on the right-hand side of each equation are synchronous with the field component solved on the left-hand side. But they can be greatly simplified. For the first sub-step, this is done by substituting the expressions of (1d-f) for the *H*-field components evaluated at time step *n+1/2* into the *E*-field updating equations of (1a-c). This yields new updating equations for all *E*-field components. As an example, Eq. (3) is the new updating equation for the E_x component.

Similarly, for the second sub-step, this is done by substituting the expressions of (2d-f) for the *H*-field components evaluated at time step *n+1* into the *E*-field updating equations of (2a-c). This yields new updating equations for all *E*-field components at the time step *n+1*.

As an example, Eq. (4) is the new updating equation for the E_x field component.

$$
\begin{aligned}
&(1+\frac{C_b\big|_{i,j+1/2,k} D_b\big|_{i,j+1/2,k-1/2}}{\Delta hy_{i+1/2,j,k}\Delta y_{i,j+1/2,k-1/2}}+\frac{C_b\big|_{i,j+1/2,k} D_b\big|_{i,j+1/2,k+1/2}}{\Delta hy_{i+1/2,j,k}\Delta y_{i,j+1/2,k+1/2}})E_x\big|^{n+1/2}_{i+1/2,j,k}\\
&-\frac{C_b\big|_{i,j+1/2,k} D_b\big|_{i+1/2,j-1/2,k}}{\Delta hy_{i+1/2,j,k}\Delta y_{i+1/2,j-1/2,k}}E_x\big|^{n+1/2}_{i+1/2,j-1,k}\\
&-\frac{C_b\big|_{i,j+1/2,k} D_b\big|_{i+1/2,j+1/2,k}}{\Delta hy_{i+1/2,j,k}\Delta y_{i+1/2,j+1/2,k}}E_x\big|^{n+1/2}_{i+1/2,j+1,k}\\
&=C_a\big|_{i+1/2,j,k}E_x\big|^{n}_{i+1/2,j,k}\\
&-C_b\big|_{i+1/2,j,k}\left[\frac{H_y\big|^{n}_{i+1/2,j,k+1/2}-H_y\big|^{n}_{i+1/2,j,k-1/2}}{\Delta hz_{i+1/2,j,k}}\right] \qquad (3)\\
&+C_b\big|_{i+1/2,j,k}\left[\frac{H_z\big|^{n}_{i+1/2,j+1/2,k}-H_z\big|^{n}_{i+1/2,j-1/2,k}}{\Delta hy_{i+1/2,j,k}}\right]\\
&-\frac{C_b\big|_{i+1/2,j,k} D_b\big|_{i+1/2,j+1/2,k}}{\Delta hy_{i+1/2,j,k}\Delta x_{i+1/2,j+1/2,k}}\left[E_y\big|^{n}_{i+1,j+1/2,k}-E_y\big|^{n}_{i,j+1/2,k}\right]\\
&+\frac{C_b\big|_{i+1/2,j,k} D_b\big|_{i+1/2,j-1/2,k}}{\Delta hy_{i+1/2,j,k}\Delta x_{i+1/2,j-1/2,k}}\left[E_y\big|^{n}_{i+1,j-1/2,k}-E_y\big|^{n}_{i,j-1/2,k}\right]
\end{aligned}
$$

$$
\begin{aligned}
&(1+\frac{C_b\big|_{i,j+1/2,k} D_b\big|_{i,j+1/2,k-1/2}}{\Delta hz_{i+1/2,j,k}\Delta z_{i,j+1/2,k-1/2}}+\frac{C_b\big|_{i,j+1/2,k} D_b\big|_{i,j+1/2,k+1/2}}{\Delta hz_{i+1/2,j,k}\Delta z_{i,j+1/2,k+1/2}})E_x\big|^{n+1}_{i+1/2,j,k}\\
&-\frac{C_b\big|_{i,j+1/2,k} D_b\big|_{i+1/2,j,k-1/2}}{\Delta hz_{i+1/2,j,k}\Delta z_{i+1/2,j,k-1/2}}E_x\big|^{n+1}_{i+1/2,j,k-1}\\
&-\frac{C_b\big|_{i,j+1/2,k} D_b\big|_{i+1/2,j,k+1/2}}{\Delta hz_{i+1/2,j,k}\Delta z_{i+1/2,j,k+1/2}}E_x\big|^{n+1}_{i+1/2,j,k+1}\\
&=C_a\big|_{i+1/2,j,k}E_x\big|^{n+1/2}_{i+1/2,j,k}\\
&-C_b\big|_{i+1/2,j,k}\left[\frac{H_y\big|^{n+1/2}_{i+1/2,j,k+1/2}-H_y\big|^{n+1/2}_{i+1/2,j,k-1/2}}{\Delta hz_{i+1/2,j,k}}\right] \qquad (4)\\
&+C_b\big|_{i+1/2,j,k}\left[\frac{H_z\big|^{n+1/2}_{i+1/2,j+1/2,k}-H_z\big|^{n+1/2}_{i+1/2,j-1/2,k}}{\Delta hy_{i+1/2,j,k}}\right]\\
&-\frac{C_b\big|_{i+1/2,j,k} D_b\big|_{i+1/2,j+1/2,k}}{\Delta hz_{i+1/2,j,k}\Delta x_{i+1/2,j+1/2,k}}\left[E_z\big|^{n+1/2}_{i+1,j,k+1/2}-E_z\big|^{n+1/2}_{i,j,k+1/2}\right]\\
&+\frac{C_b\big|_{i+1/2,j,k} D_b\big|_{i+1/2,j-1/2,k}}{\Delta hz_{i+1/2,j,k}\Delta x_{i+1/2,j-1/2,k}}\left[E_z\big|^{n+1/2}_{i+1,j,k-1/2}-E_z\big|^{n+1/2}_{i,j,k-1/2}\right]
\end{aligned}
$$

Eq. (3) shows that the E_x field component at the node (i+*1/2,j,k*) is coupled with those at the node (i+*1/2,j+1,k*) and the node (i+*1/2,j-1,k*). This leads to a set of simultaneous equations for E_x when written for each j coordinate along a y-directed line through the space lattice. The matrix associated with this system is tridiagonal, and hence, can be easily solved. This process is repeated for each y-cut through the grid where E_x components are located. All E field components in both sub-steps have the same characteristics.

The H field updating equations (1d-f) and (2d-f) are now fully explicit because all of their required E field component data at the time step n+1/2 and time step n+1 are available after all new E field updating equations have been solved in the manner described above.

For the uniform grid ADI-FDTD algorithm, the Eq. (3) and (4) can be further simplified by setting $\Delta hx=\Delta x$, $\Delta hy=\Delta y$ and $\Delta hz=\Delta z$.

III. Numerical Investigation

Since the ADI-FDTD is always stable [2,3], the selection of the time step is no longer restricted by stability, but the relative error of the ADI-FDTD scheme increases with the time step chosen. To compare the performance of the ADI-FDTD and conventional FDTD algorithms, we have solved the two numerical examples presented below. All simulations were performed on a 450 MHz Pentium-II with 128MB of memory under Windows 2000. The CPU times do not include the time used for Discrete Fourier Transform (DFT) calculations.

A. Cavity Half-filled With Dielectric Material

A 7.112mm x 3.556mm x 5.334mm rectangular cavity was modeled with both ADI-FDTD and conventional FDTD. One half of the cavity was filled with air and the other half with the dielectric material of relative permittivity 2.22. For both algorithms, a uniform mesh with Δl =0.3556mm was used, yielding a mesh with 20×10×15 cells. A time step Δt_{FDTD}=0.593ps was chosen for the conventional FDTD, while several different time steps Δt_{ADI} were used with the ADI-FDTD to check its accuracy. The physical simulation time of 10,000Δt_{FDTD} was kept the same in all cases. Fig. 2 shows the relative error in the first two resonant frequencies obtained with ADI-FDTD. The relative error affecting the conventional FDTD algorithm was virtually the same as for ADI-FDTD when the time steps were identical ($\Delta t_{ADI}=\Delta t_{FDTD}$). Fig. 2 also shows the ratio of the CPU-time required by ADI-FDTD and that required by the conventional FDTD. Fig. 2 shows that although the ADI-FDTD algorithm is unconditionally stable, the relative error quickly increases with the length of the time step. A reduction in the number of time steps and hence, in the CPU time, is obtained at the expense of a larger computational error.

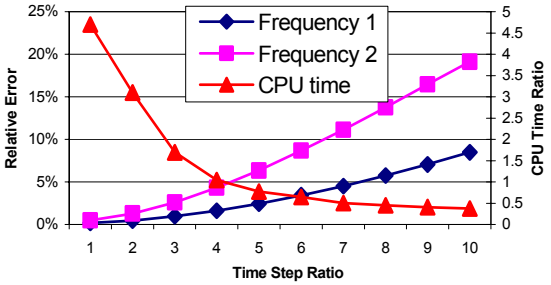

Fig. 2. Relative error in resonant frequencies, and CPU time ratio of ADI-FDTD, vs. the time step ratio $\Delta t_{ADI}/\Delta t_{FDTD}$. (The analytical values of the resonant frequencies are 34.87GHz and 49.70GHz, respectively)

B. Inhomogeneous Rectangular Cavity With Two Fins

The conventional FDTD algorithm with a non-uniform mesh yields better accuracy than uniform meshing when field singularities are present. Unfortunately, the maximum stable time step is still limited by the smallest spatial discretization interval. We compared the performance of the regular FDTD and ADI-FDTD algorithms with a graded mesh as well.

The geometry of the cavity is shown in Fig. 3. The cavity was discretized by a smoothly graded mesh shown in Fig. 4. The mesh size was 30x60x30 cells.

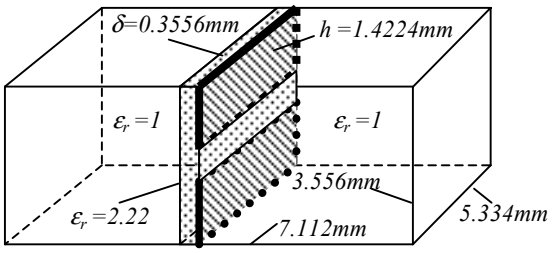

Fig. 3 Inhomogeneous rectangular finline cavity

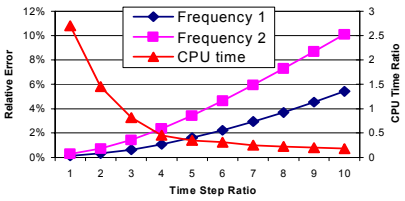

Fig. 4 The graded mesh in the x-y cross-section

Fig. 5 shows the relative error in the first two resonant frequencies obtained with ADI-FDTD. However, in this case, the computational resonant frequencies obtained by the conventional FDTD algorithm were considered as the reference values. For comparison, the ratio of the required CPU-times for ADI-FDTD and conventional FDTD is also shown in Fig. 5. Both the relative error and the CPU time are greatly reduced in the graded mesh. But the tendencies of all curves are similar to those obtained in the uniform mesh. When the ADI-FDTD is run with about 3 to 5 times the time step of the conventional FDTD for the same mesh size, the accuracy of both algorithms is about the same.

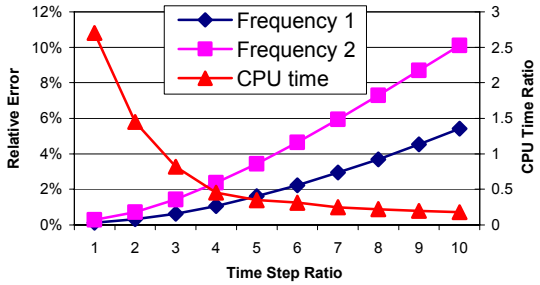

Fig. 5. Relative error in resonant frequency and CPU time ratio of ADI-FDTD, vs. time step ratio $\Delta t_{ADI}/\Delta t_{FDTD}$. (The values of the above resonant frequencies obtained by conventional FDTD are 39.52GHz and 54.03GHz, respectively)

IV. Conclusion

A 3D ADI-FDTD algorithm has been implemented and compared with the conventional FDTD algorithm by using uniform and graded meshes. The ADI-FDTD algorithm is unconditionally stable, and the selection of the time step is not restricted by stability. However, the relative error in the ADI-FDTD result quickly increases with the increase of time step. The CPU time saving over conventional FDTD is not dramatic when the same computational accuracy is required. Furthermore, the memory requirement of the ADI-FDTD algorithm is about twice that of the conventional FDTD for the same mesh. Therefore, the choice between ADI-FDTD and regular FDTD depends mainly on the size of the acceptable error.

References

[1] F. Zheng, Z. Chen and J. Zhang, "Development of Three-Dimensional Unconditionally Stable Finite-Difference Time-Domain Methods", *2000 IEEE MTT-S Int. Microwave Symp. Dig.*, pp.1117-1120, May, 2000.

[2] F. Zheng, Z. Chen and J. Zhang, "Toward the Development of Three-Dimensional Unconditionally Stable Finite-Difference Time-Domain Method", *IEEE Trans. Microwave Theory and Tech.*, vol. 48, no. 9, pp. 1550-1558, Sept. 2000.

[3] T. Namiki, "3-D ADI-FDTD Method—Unconditionally Stable Time-Domain Algorithm for Solving Full Vector Maxwell's Equations", *IEEE Trans. Microwave Theory and Tech.*, vol. 48, no. 10, pp. 1743-1748, Oct. 2000.